Highlights of Spanish Astrophysics XII, Proceedings of the XVI Scientific Meeting of the Spanish Astronomical Society held on July 15 - 19, 2024, in Granada, Spain. M. Manteiga, F. González Galindo, A. Labiano Ortega, M. Martínez González, N. Rea, M. Romero Gómez, A. Ulla Miguel, G. Yepes, C. Rodríguez López, A. Gómez García and C. Dafonte (eds.), 2025

A catalogue of Mg, Ca and C abundances from the X-shooter Spectral Library: benchmark for improving the modelling of stellar population models

Santos-Peral, P.[1,2], Sánchez-Blázquez, P.[1,2], Vazdekis, P.[3,4], Palicio, P.A.[5], Recio-Blanco, A.[5], Knowles, A.T.[3,4,6], Gaspar-Gorostieta, I.A.[3,4], and Allende-Prieto, C.[3,4]

[1] Departamento de Física de la Tierra y Astrofísica, Universidad Complutense de Madrid, 28040 Madrid, Spain
[2] Instituto de Física de Partículas y del Cosmos IPARCOS, Facultad de CC Físicas, Universidad Complutense de Madrid, 28040 Madrid, Spain
[3] Instituto de Astrofísica de Canarias, E-38200 La Laguna, Tenerife, Spain
[4] Departamento de Astrofísica, Universidad de La Laguna, E-38205, Tenerife, Spain
[5] Université Côte d'Azur, Observatoire de la Côte d'Azur, CNRS, Laboratoire Lagrange, Bd de l'Observatoire, CS 34229, 06304 Nice cedex 4, France
[6] Data Science Research Centre, Liverpool John Moores University, Liverpool, L3 3AF, UK

Abstract

The completeness of stellar spectral libraries across all evolutionary phases, parameter space and chemical abundances, is essential to build more sophisticated stellar population synthesis models to decode information from galaxy spectra.
On the one hand, due to distinct nucleosynthesis channels, the comparison between magnesium and calcium can provide relevant information to understand the evolution of asymptotic giant branch (AGB) stars, the IMF (the relative production of Mg versus Ca in core-collapse supernovae varies with the mass of the progenitor), or the SFH (Star Formation History). On the other hand, determining carbon abundances helps assess the contribution of AGB stars to the total infrared luminosity, with significant implications for estimating the stellar masses and ages of high-redshift galaxies.
In this context, we use the X-shooter Spectral Library (XSL) as a benchmark to train advanced stellar population models, incorporating both alpha and carbon-enhancements. The XSL, with a moderately high resolution (R $\sim$ 10000) and a large wavelength coverage (300-2480 nm), represents a huge improvement over previous empirical stellar spectral libraries. For this purpose, we employed the automated abundance estimation procedure GAUGUIN to derive precise and accurate magnesium and calcium abundances from a diverse sample of stars well distributed across the Hertzsprung-Russell (HR) diagram. Additionally, preliminary results indicate promising carbon abundance estimates.
In conclusion, the provided XSL abundance catalogue ([1]) is suitable for improving the modelling of evolutionary stellar population models with empirical α-enhancements, and its implementation will allow us to study small galaxies with nearly solar-scaled abundances in the sub-solar, as well as metal-poor metallicity regimes and massive galaxies with enhanced [α/Fe] in the high-metallicity regime, with an unprecedented precision. This will significantly contribute to the quality of research of external galaxies' abundances, with special focus on current and next-generation of field spectrographs such as MEGARA, WEAVE, 4MOST, or TARSIS.

1 Introduction

Empirical stellar spectral libraries are key for the development of stellar population synthesis models to unveil the unresolved stellar populations from galactic spectra [2].

The X-shooter Spectral Library[1] (XSL [3]) is an empirical stellar spectral library that comprises 830 spectra for 683 stars, observed at a moderate-resolution (R $\sim$ 10000), covering the whole Kiel diagram homogeneously with a wide range of chemical compositions. Three spectral ranges are observed: UVB (ultraviolet-blue; 300-556 nm), VIS (visible; 533-1020 nm), and NIR (near-infrared; 994-2480 nm), making the XSL a reference stellar library in the optical and NIR.

Complementary high-precision chemical abundances are essential to infer the properties and enrichment processes involved in the galaxy formation and evolution: star formation rate

[1] `http://xsl.astro.unistra.fr`

(SFR), initial mass function (IMF), production of elements (yields) by stars with different masses and metallicities, or the gas evolution (migration, dilution, outflows).

The main objective of this work is to provide reliable [α/Fe] (public catalogue published in [1]) and carbon abundances for one of the most complete empirical stellar libraries in the literature. In this work, we present a detailed spectroscopic analysis of the Mg, Ca and C abundance estimation for a large variety of 616 parametrised stars [4]: 2900 < $T_{\rm eff}$ < 38000 K, 0 < log(g) < 5.7 cm s^{-2}, and -2.5 < [Fe/H] < +1.0 dex.

2 Methodology

After a careful visualisation, we derived and analysed the chemical abundances from individual spectral lines in the optical and NIR range via the optimised spectrum synthesis algorithm GAUGUIN, mainly developed in the framework of the *Gaia*/RVS analysis pipeline [5].

The abundance analysis was performed using three magnesium spectral lines in the optical range, three near-infrared calcium lines, and three clean CH bands for the carbon abundance estimates, as indicated in Table 1. For the selection of our analysed lines, we firstly referred to the work of [6], who performed an extensive spectroscopic analysis of nine different magnesium lines in the optical range. We also followed the work of [5], who analysed the same Ca II IR triplet for *Gaia* DR3. The clean CH bands were based on [7]. We ensured that chemical abundances could be properly measured from any stellar type and at low-medium spectral resolution (neither weak nor blended atomic lines).

Table 1: Magnesium, calcium, and carbon lines/regions selected in the analysis.

	Mg I (Å):	
5167.3	5172.7	5183.6
	Ca II (Å):	
8498.02	8542.09	8662.14
	CH bands (Å):	
4279.2-4281.6	4301.5-4303.4	4307.1-4308.8

3 X-shooter catalogue of chemical abundances

3.1 [Mg/Fe] & [Ca/Fe] (Santos-Peral et al. 2023)

In [1] we published the magnesium and calcium abundances, with their associated internal uncertainty (around $\sim$ 0.02 dex, always smaller than 0.1 dex), for 192 and 217 stars, respectively. The complete abundance catalogue is available in electronic form (Vizier DOI: 10.26093/cds/vizier.36720166). In the following figures, we summarise the X-shooter stellar sub-sample of 174 stars from which we provide reliable [Mg/Fe] and [Ca/Fe] abundances.

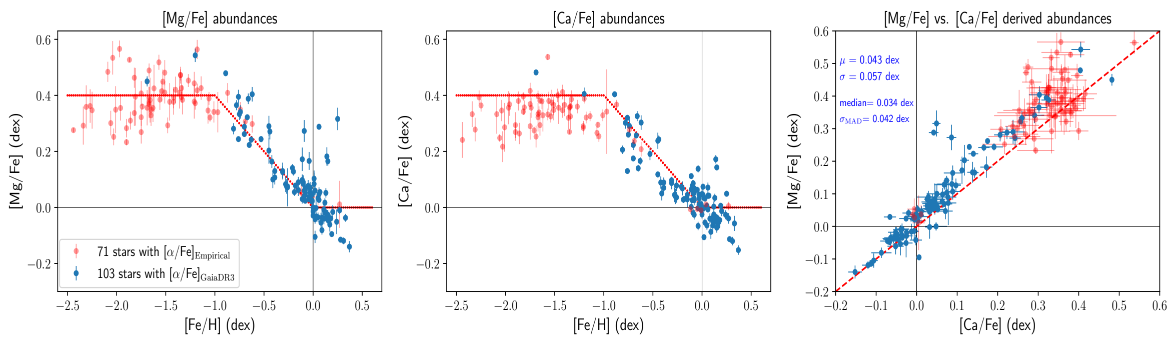

Figure 1: Comparison of the derived stellar abundance ratios from the final X-shooter stellar sample with reliable [Mg/Fe] and [Ca/Fe] abundances. *Left and middle panels*: [Mg/Fe] and [Ca/Fe] as a function of [Fe/H], respectively. *Right panel*: direct comparison [Mg/Fe] vs. [Ca/Fe].

Figure 1 illustrates each element abundance ratios [X/Fe] relatively to the stellar metallicity [Fe/H] (left and middle panels), and their direct comparison (right panel). As can be seen, both abundance ratios reproduce a plateau in the metal-poor regime ([Fe/H] $\leq$ -1.0 dex) followed by a decrease even at supersolar metallicities ([Fe/H] $>$ 0.0 dex) due to the contribution from Type Ia SNe. This behaviour is typical for α-element evolution and is in perfect agreement with the predictions of Galactic chemical evolution models (e.g. [8]). In addition, we measured relatively higher magnesium abundances in comparison with calcium values (with a systematic difference at $\sim$ 0.034 dex, see right panel), which is more easily noticeable for metal-poor stars ([Fe/H] $\leq$ -1.0 dex) where the [Mg/Fe] abundance shows a larger dispersion. This behaviour has been previously reported in the literature from both observational and theoretical points of view, which could be explained by a possible mass or metallicity dependence in the Ca yields of core-collapse supernovae Type II SNe (e.g. [9], [10]).

Figure 2 shows the covered parameters in the Kiel diagram by the XSL stellar subsample with measurements in both elements. We successfully obtained chemical abundances for a wide range of stellar types, including dwarfs and giants, well distributed in effective temperature (4000 $<$ T_{eff} $<$ 6500 K) and metallicity (-2.5 $<$ [Fe/H] $<$ +0.4 dex). The completeness of the provided catalogue in the atmospheric parameter and chemical space is ideal for improving the development of evolutionary stellar population synthesis models in the near future for the analysis of external galaxies abundances.

3.2 [C/Fe]

Preliminarily, we have also characterised the carbon abundances in the XSL sample, using the CH bands listed in Table 1, based on predictions from the stellar atmosphere models computed by [11]. We were able to measure reliable [C/Fe] estimates, showing a good spectral fit and compatible derived carbon abundances from each analysed spectral region of the same star.

Figure 3 illustrates the measured stellar [C/Fe] abundance with respect to their metallicity

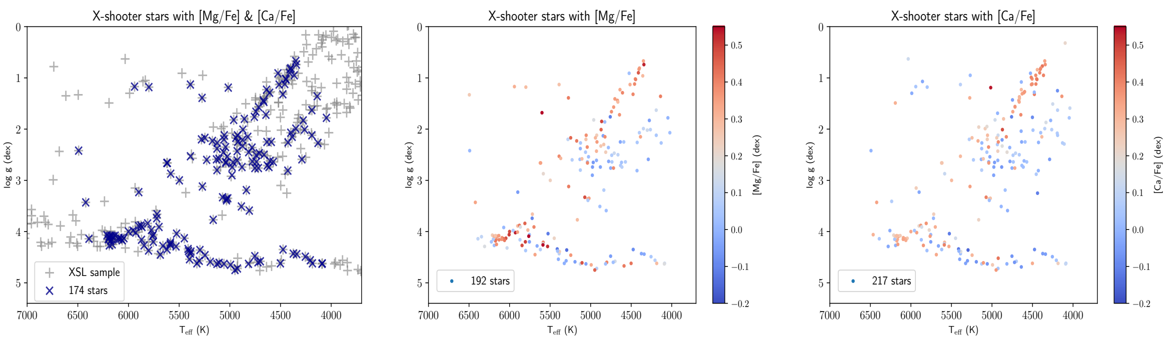

Figure 2: Kiel diagrams of the final X-shooter stellar sample with reliable [Mg/Fe] and [Ca/Fe] abundance measurements. *Left panel*: stars chemically characterised with [Mg/Fe] and [Ca/Fe] abundances (blue crosses) over the whole analysed X-shooter sample in this work (grey crosses). *Middle and right panels*: stars with [Mg/Fe] and [Ca/Fe] estimates, colour-coded by the element abundance respectively.

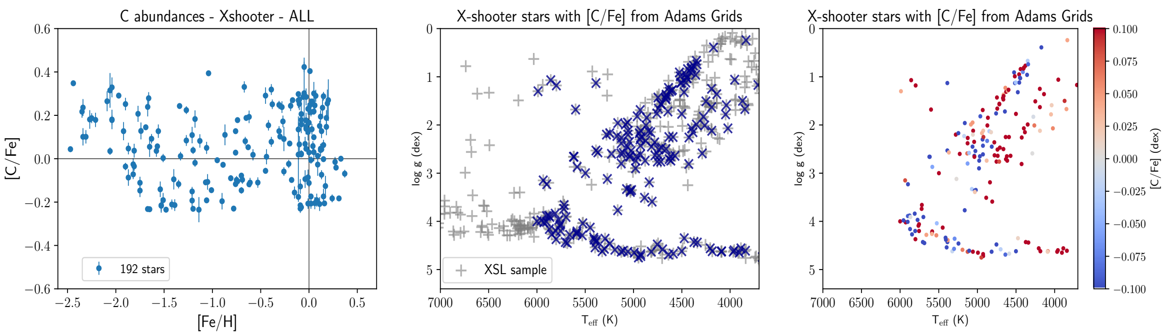

Figure 3: *Left panel*: Stellar [C/Fe] abundances as a function of [Fe/H]. *Middle panel*: stars distributed in the Kiel diagram with a [C/Fe] abundance estimate (blue crosses) over the whole analysed X-shooter sample (grey crosses). *Right panel*: same as middle panel, colour-coded by the carbon abundance.

(left panel), and the covered region in the Kiel diagram (middle and right panel). We do not observe any trend with stellar parameters ($T_{\rm eff}$, logg, [Fe/H]). As shown in Fig. 3, the [C/Fe] abundances describe a dispersed ($\sigma_{\rm [C/Fe]} \sim 0.2$ dex) flat trend around [C/Fe] ~ 0.0 dex all along the covered metallicity range (-2.5 < [Fe/H] < +1.0 dex). The only remarkable feature is the observed convex curve at low [C/Fe] abundances around [Fe/H] $\sim$ -0.5 dex, which seems to be present in some previous observational studies in the literature (e.g. APOGEE DR16 [12]).

As discussed in Sect. 3.1, we measured carbon abundances for different stellar types, well distributed in the parameter space, ideal for training and include carbon-enhancements in stellar population models. This could be employed to study the discrepancies between the observed and predicted CO bands. For instance, the CO-strong environment-dependent features observed in massive ETGs remains as one of the biggest challenges for understanding their stellar content and implications on their formation within varying galaxy cluster types (e.g. [13]).

Acknowledgments

The authors sincerely thank Sara R. Berlanas and David Aguado, main scientific organisers of the symposium *"The involvement of the Spanish community in WEAVE: from survey preparation to first science results"*, the opportunity to show our project to the community. P.S.P acknowledges financial support by the Spanish Ministry of Science and Innovation through the research grants PID2019-107427GB-C31 and PID2022-138855NB-C31, and also financial support by the European Union – NextGenerationEU under a Margarita Salas contract.

References

[1] Santos-Peral, P., Sánchez-Blázquez, P., Vazdekis, A., & Palicio, P. A. 2023, A&A, 672, A166

[2] Conroy, C. 2013, ARA&A, 51, 393

[3] Gonneau, A., Lyubenova, M., Lançon, A., et al. 2020, A&A, 634, A133

[4] Arentsen, A., Prugniel, P., Gonneau, A., et al. 2019, A&A, 627, A138

[5] Recio-Blanco, A., de Laverny, P., Palicio, P. A., et al. 2023, A&A, 674, A29

[6] Santos-Peral, P., Recio-Blanco, A., de Laverny, P., Fernández-Alvar, E., & Ordenovic, C. 2020, A&A, 639, A140

[7] Suárez-Andrés, L., Israelian, G., González Hernández, J. I., et al. 2017, A&A, 599, A96

[8] Palla, M., Santos-Peral, P., Recio-Blanco, A., & Matteucci, F. 2022, A&A, 663, A125

[9] Zasowski, G., Schultheis, M., Hasselquist, S., et al. 2019, ApJ, 870, 138

[10] Kobayashi, C., Umeda, H., Nomoto, K., Tominaga, N., & Ohkubo, T. 2006, ApJ, 653, 1145

[11] Knowles A. T., Sansom A. E., Allende Prieto C., Vazdekis A., 2021, MNRAS, 504, 2286

[12] Jönsson, H., Holtzman, J. A., Allende Prieto, C., et al. 2020, AJ, 160, 120

[13] Eftekhari, E., La Barbera, F., Vazdekis, A., Allende Prieto, C., Knowles, A. T., 2022, MNRAS, 512, 378